# LDPC coding for bursty optical channels



Citation for the original published paper (version of record):
Cui, H., Carlsson, M., Agrell, E. (2025). LDPC coding for bursty optical channels. European Conference on Optical Communication, ECOC: 707-710.
http://dx.doi.org/10.1109/ECOC66593.2025.11263240

# LDPC coding for bursty optical channels

Han Cui, Magnus Karlsson, Erik Agrell

Chalmers University of Technology, Sweden, hancu@chalmers.se

***Abstract*** *We propose an LDPC decoding scheme for bursty residual phase noise channels, using Viterbi-based channel state estimation and burst-aware LLRs. Simulations show improved bit and packet error rates over conventional schemes with and without interleaving.* 

## Introduction

In optical communication systems, time-varying impairments arising from system components[1], lightwave propagation[2],[3], and digital signal processing (DSP)[4]can lead to burst errors, which severely degrade overall system performance.

Interleaving is a common method for mitigating burst errors by dispersing consecutive bits over time, making the channel appear memoryless[5]. Although effective, it introduces latency and may reduce channel capacity[6]. However, most network protocols detect and retransmit errors at the packet level[7], so even a few scattered bit errors can lead to the loss of multiple packets. Therefore, interleaving may increase the packet error rate (PER) under severe burst conditions.

Low-density parity-check codes (LDPC) are widely used in optical communication for the strong error correction and near-capacity performance[8]. The performance of LDPC relies on the accuracy of soft information, such as log-likelihood ratios (LLRs). The LLRs must be well matched to the channel conditions, including bursty noise and other memory effects for optimal performance.

Certain physical-layer phenomena, such as sudden phase disturbances induced by lightning strikes[9], laser instability[10], and phase recovery imperfections[11], can cause bursty residual phase noise, which challenges conventional equalization and decoding. While Viterbi-based channel state estimation has been studied in wireless fading scenarios[12], its use for residual phase noise in optical systems has not been reported. This work addresses this gap by proposing a joint burst-aware LDPC (JBA-LDPC) decoding scheme that combines Viterbi-based state estimation with burst-aware LLR calculation. The method is evaluated under various burst conditions, with and without interleaving. Simulation results show improvements in both bit error rate (BER) and PER compared with traditional schemes where channel state information is unavailable.

## Channel Model

Assuming that all other impairments are perfectly compensated, this study focuses on bursty residual phase noise and additive white Gaussian noise (AWGN). The channel can be modeled as

$$Y = Xe^{j\theta} + N, \tag{1}$$

where $X$ and $Y$ are the transmitted and received complex signals, respectively. $N$ is the AWGN with zero mean and variance $\sigma^2$, and $\theta$ is the residual phase noise, which follows a Gaussian distribution of zero mean and variance $\sigma_S^2$.

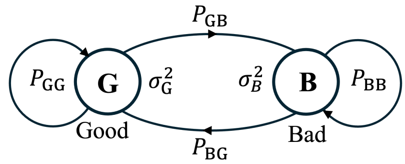


**Fig. 1:** State diagram of the Gilbert–Elliott (GE) model

To represent a bursty phase noise channel, a Gilbert–Elliott (GE) model[6],[13] is used as shown in Fig. 1. There are two states $S$ in a GE model: good $(\mathrm{G})$ and bad $(\mathrm{B})$. The two states correspond to different severities of the residual phase noise. The residual phase noise in the $\mathrm{G}$ state has a variance of $\sigma_S^2 = \sigma_{\mathrm{G}}^2$, while the $\mathrm{B}$ state has a significantly larger variance denoted by $\sigma_S^2 = \sigma_{\mathrm{B}}^2$. The state transition probabilities are $P_{\mathrm{GB}}$ from $\mathrm{G}$ to $\mathrm{B}$ and $P_{\mathrm{BG}}$ from $\mathrm{B}$ to $\mathrm{G}$. Thus, the probabilities of remaining in the same state are $P_{\mathrm{GG}} = 1 - P_{\mathrm{GB}}$ and $P_{\mathrm{BB}} = 1 - P_{\mathrm{BG}}$. The steady-state probability, which is the long-term average probability of being in each state, can be calculated as

$$P_{\mathrm{G}} = \frac{P_{\mathrm{BG}}}{P_{\mathrm{GB}} + P_{\mathrm{BG}}}, \tag{2}$$

$$P_{\mathrm{B}} = \frac{P_{\mathrm{GB}}}{P_{\mathrm{GB}} + P_{\mathrm{BG}}}. \tag{3}$$

Compared with the normal AWGN channel, residual phase noise in (1) requires a modified likelihood function, where $p(Y|X)$ denotes the likelihood of receiving $Y$ given $X$. As the exact form is intractable, two approximation methods can be employed[14]: the linear transform (LT) and the bilinear transform (BLT). Additionally, the channel state should be considered when calculating the likelihood in bursty channels, meaning that $p(Y|X)$ should be replaced by $p(Y|X, S)$. Thus, the LT- and BLT-based likelihood functions, along with the channel state, can be respectively given by

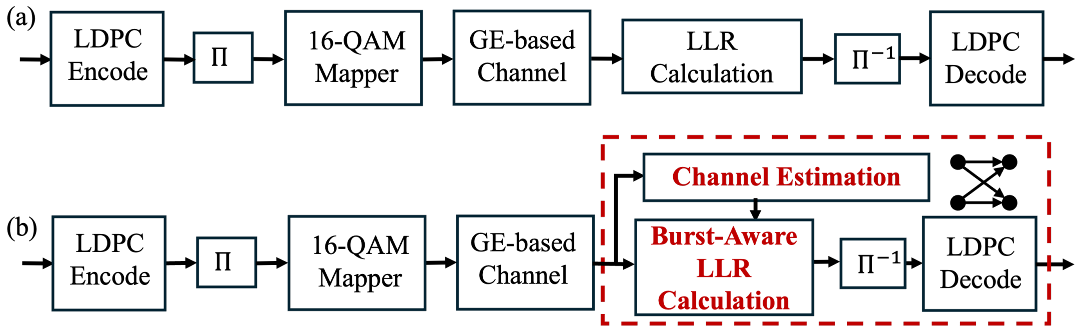


**Fig. 2:** Schematic diagram of the (a) baseline LDPC and (b) joint burst-aware (JBA) LDPC encoding and decoding processes in 16-QAM transmission systems with interleaving ($\Pi$)

$$\log\left(p(Y|X,S)\right) \approx -\frac{1}{\sigma^2}|Y-X|^2 + \frac{2\sigma_S^2}{\sigma^4+2\sigma^2\sigma_S^2|X|^2}\left(\Im[X^*Y]\right)^2 - \frac{1}{2}\log\left(\sigma^2+2\sigma_S^2|X|^2\right)+C, \tag{4}$$

$$\log\left(p(Y|X,S)\right) \approx -\frac{1}{\sigma^2}|Y-X|^2 + \frac{4\sigma_S^2}{2\sigma^4+\sigma^2\sigma_S^2|X+Y|^2}\left(\Im[X^*Y]\right)^2 - \frac{1}{2}\log\left(\sigma^2+\frac{\sigma_S^2}{2}|X+Y|^2\right)+C, \tag{5}$$

where $C$ is a constant, independent of $X$ and $Y$. The first term of (4) and (5) gives the likelihood function for the AWGN channel. The noise variance $\sigma_S^2$ should be replaced by $\sigma_{\mathrm{G}}^2$ or $\sigma_{\mathrm{B}}^2$, depending on the channel state.

### Joint Burst-Aware LDPC Decoding

To effectively mitigate the impact of bursty residual phase noise on LDPC decoding performance, we propose the JBA-LDPC decoding scheme as shown in Fig. 2(b). The proposed scheme consists of two components, which are a two-state Viterbi-based channel state estimation algorithm and a burst-aware LLR calculation. The following sections describe each component in detail.

### Viterbi-Based Channel State Estimation

In the Viterbi-based channel state estimation algorithm, two states in the trellis represent the $\mathrm{G}$ state and the $\mathrm{B}$ state, respectively. Different branches in the trellis represent transitions between states. For example, the branch labeled (1) in Fig. 3 indicates a transition from state $S_{i-1}=\mathrm{G}$ to state $S_i=\mathrm{G}$. At time $i$, the branch metric can be calculated as

$$BM_i = p\left(Y_i|S_i\right)\cdot P\left(S_i|S_{i-1}\right), \tag{6}$$

where $Y_i$ and $S_i$ are the received signal and the channel state at time $i$, respectively. The term

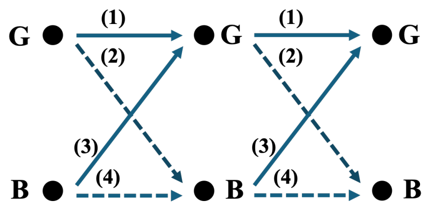


**Fig. 3:** Trellis of two-state Viterbi-based channel state estimation algorithm

$P\left(S_i|S_{i-1}\right)$ represents the state transition probability in the GE model. Since the transmitted signal is unavailable, $p\left(Y_i|S_i\right)$ can be calculated as

$$p(Y_i|S_i) = \sum_X p\left(Y_i|X,S_i\right)\cdot P(X). \tag{7}$$

### Burst-Aware LLR Calculation

To perform LDPC decoding of a received signal $Y$, the LLR for each transmitted bit must be computed. The burst-aware LLR can calculate as

$$LLR_m\left(Y\right) = \log\left(\frac{\sum\limits_{X\in\mathcal{X}_0^m} p(Y|X,S)P(X)}{\sum\limits_{X\in\mathcal{X}_1^m} p(Y|X,S)P(X)}\right). \tag{8}$$

Here, $\mathcal{X}_0^m$ and $\mathcal{X}_1^m$ denote the sets of modulation symbols where the $m$-th bit of $X$ is 0 or 1, respectively. Since a uniform prior $P(X)=1/M$ is assumed, where $M$ is the modulation order, $P(X)$ can therefore be omitted from (7) and (8) as it contributes equally. The channel state information can be obtained after the Viterbi-based channel state

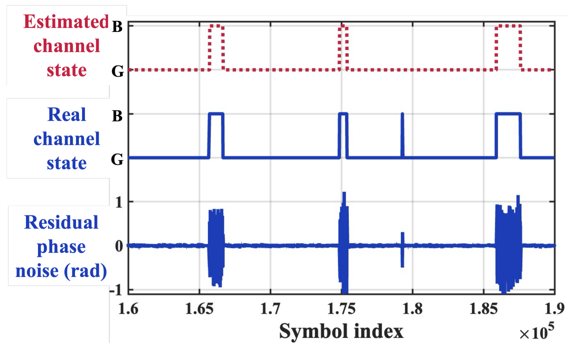


**Fig. 4:** Viterbi-based channel state estimation at SNR $=13$dB with $\sigma_{\mathrm{G}}^2=0.0003$ and $\sigma_{\mathrm{B}}^2=0.1218$, and BLT-based likelihood function.

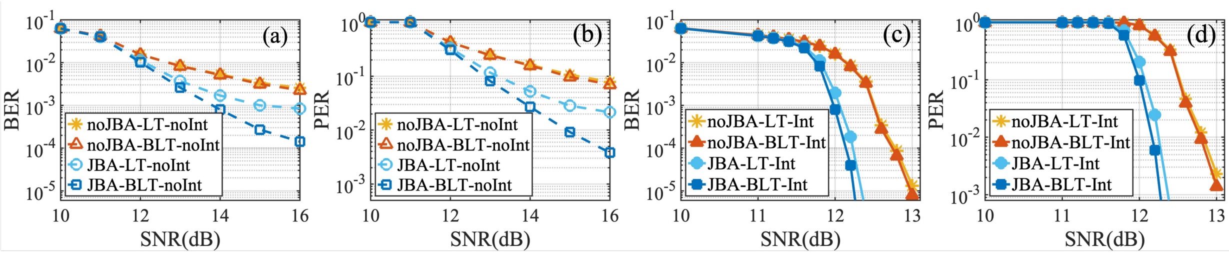


**Fig. 5:** Bit and packet error rates of different SNR are shown for a fixed $\sigma_{\mathrm{G}}^2 = 0.0003$ and $\sigma_{\mathrm{B}}^2 = 0.1218$. (a)BER performance without interleaving; (b)PER performance without interleaving; (c)BER performance with interleaving; (d)PER performance with interleaving.

estimation algorithm. In this way, the LDPC decoder receives LLRs that more accurately reflect the channel conditions compared to those computed without channel state information, thereby enhancing robustness against bursty phase noise.

As a baseline when channel state information is unavailable, the likelihood functions reduce from $p(Y|X,S)$ to $p(Y|X)$ by replacing $\sigma_S^2$ with an effective noise variance $\sigma_{\mathrm{eff}}^2$ in (4) and (5). This effective variance is the average of the noise variances in the $\mathrm{G}$ and $\mathrm{B}$ states, using their respective steady-state probabilities as weights, and can be expressed as

$$\sigma_{\mathrm{eff}}^2 = \sigma_{\mathrm{G}}^2 \cdot P_{\mathrm{G}} + \sigma_{\mathrm{B}}^2 \cdot P_{\mathrm{B}}. \qquad (9)$$

## Simulation Setup and Results Analysis

Monte Carlo simulations were performed for LDPC-coded 16-QAM transmission over a channel affected by AWGN and bursty residual phase noise. The LDPC code followed the IEEE 802.3ca standard, with a codeword length of 17664 bits and 14592 information bits[15]. The total number of information bits was 58368000, corresponding to 114,000 packets, each packet consisting of 512 bits[16]. The GE phase noise model was set with transition probabilities $P_{\mathrm{GB}} = 2 \times 10^{-4}$ and $P_{\mathrm{BG}} = 2 \times 10^{-3}$, corresponding to an average burst length of 500 symbols. In interleaved scenarios, the depth of the interleaver was set to 1024, which is significantly longer than the average burst length, to mitigate the impact of burst errors.

Fig. 4 illustrates the effectiveness of the proposed Viterbi-based channel state estimation. The estimator effectively tracks most channel states, with only very short bursts occasionally missed. Its overall consistency with the actual state supports reliable LLR calculation and LDPC decoding.

Fig. 5 shows the BER and PER performance as a function of signal-to-noise ratio (SNR). Eight decoding schemes were compared, each defined by a unique combination of three dimensions. First, joint burst-aware decoding is either applied (JBA) or not (noJBA). Second, LLRs are computed using either an LT-based (LT) or a BLT-based (BLT) method. Third, interleaving is either employed (Int) or omitted (noInt). Overall, the JBA scheme based on BLT consistently achieves the best performance. JBA-BLT-noInt achieves a 1.5-dB gain over noJBA-BLT-noInt, with the comparison made at a BER of $4 \times 10^{-3}$; similarly, JBA-BLT-Int provides a 0.5-dB improvement over noJBA-BLT-Int under the same BER. In terms of PER, JBA-BLT-Int outperforms noJBA-BLT-Int by 0.7 dB at 1% PER. Without interleaving, the other three schemes, except the JBA-BLT-Int scheme, cannot achieve 1% PER target.

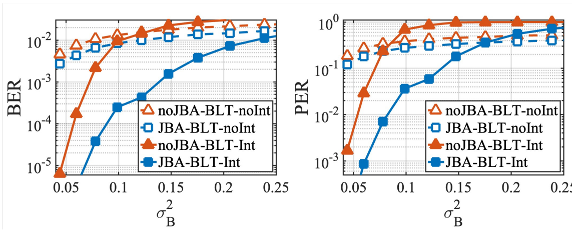


**Fig. 6:** Bit and packet error rates versus $\sigma_{\mathrm{B}}^2$ at fixed SNR $= 12$dB and $\sigma_{\mathrm{G}}^2 = 0.0003$.

Fig. 6 shows the BER and PER performance of the best-performing noJBA and JBA decoding schemes as a function of $\sigma_{\mathrm{B}}^2$. JBA-BLT-Int consistently achieves the lowest BER across all values of $\sigma_{\mathrm{B}}^2$, demonstrating superior robustness to bursty phase noise. However, here a different trend emerges for PER: when $\sigma_{\mathrm{B}}^2 < 0.17$, JBA-BLT-Int still performs best, but under more severe burst conditions, JBA-BLT-noInt performs best. This is because a single bit error leads to a full packet error, and interleaving spreads localized errors across packets. A similar trend has been observed under fixed $\sigma_{\mathrm{B}}^2$ when varying $\sigma_{\mathrm{G}}^2$.

## Conclusion

We proposed a JBA-LDPC decoding scheme for bursty residual phase noise channels, combining Viterbi-based state estimation with burst-aware LLR computation. Simulation results show that the proposed scheme consistently outperforms baseline methods in both BER and PER. Interleaving may degrade performance under severe conditions due to error dispersion, and PER is more sensitive than BER. While phase noise is used as the main example in this work, the proposed method is general and can potentially be extended to other types of bursty channel impairments, such as fast polarization drift or nonlinear crosstalk. Exploring these broader applications will be an important direction for future work.

## Acknowledgements

This research was funded by the Swedish Research Council (VR) under grants no. 2021-03709.

## References

[1] N. Iiyama, M. Fujiwara, T. Kanai, H. Suzuki, J.-i. Kani, and J. Terada, "Clock conversion for burst-mode digital coherent QPSK receivers in a PON upstream transmission with a 100-ppm clock mismatch", *Optics Express*, vol. 29, no. 2, pp. 1265–1274, 2021. DOI: 10.1364/OE.410522.

[2] M. Farsi, C. Häger, M. Karlsson, and E. Agrell, "Polarization tracking in the presence of PDL and fast temporal drift", *Journal of Lightwave Technology*, vol. 40, no. 19, pp. 6408–6416, 2022. DOI: 10.1109/JLT.2022.3194734.

[3] L. G. Cancela and J. J. Pires, "Applying the skew-normal distribution to model coherent MPI and to evaluate its impact on PAM signals", *Optical Fiber Technology*, vol. 56, pp. 1068–5200, 2020. DOI: 10.1016/j.yofte.2020.102180.

[4] K. Wu, G. Liga, J. Riani, and A. Alvarado, "Low-Complexity Soft-Decision Detection for Combating DFE Burst Errors in IM/DD Links", *Journal of Lightwave Technology*, vol. 42, no. 5, pp. 1395–1408, 2024. DOI: 10.1109/JLT.2023.3324602.

[5] W. An, M. Médard, and K. R. Duffy, "Keep the bursts and ditch the interleavers", *IEEE Transactions on Communications*, vol. 70, no. 6, pp. 3655–3667, 2022. DOI: 10.1109/TCOMM.2022.3171798.

[6] E. N. Gilbert, "Capacity of a burst-noise channel", *The Bell System Technical Journal*, vol. 39, no. 5, pp. 1253–1265, 1960. DOI: 10.1002/j.1538-7305.1960.tb03959.x.

[7] M. Nord and H. Øverby, "Packet loss rate and jitter differentiating quality-of-service schemes forasynchronous optical packet switches", *Journal of Optical Networking*, vol. 3, no. 12, pp. 866–881, 2004. DOI: 10.1364/JON.3.000866.

[8] T. Fehenberger, G. Böcherer, A. Alvarado, and N. Hanik, "LDPC coded modulation with probabilistic shaping for optical fiber systems", in *Optical Fiber Communications Conference and Exhibition (OFC)*, Los Angeles, CA, USA, 2015, pp. 1–3. DOI: 10.1364/OFC.2015.Th2A.23.

[9] P. M. Krummrich, D. Ronnenberg, W. Schairer, D. Wienold, F. Jenau, and M. Herrmann, "Demanding response time requirements on coherent receivers due to fast polarization rotations caused by lightning events", *Optics Express*, vol. 24, no. 11, pp. 12 442–12 457, 2016. DOI: 10.1364/OE.24.012442.

[10] T. N. Huynh, F. Smyth, L. Nguyen, and L. P. Barry, "Effects of phase noise of monolithic tunable laser on coherent communication systems", *Optics Express*, vol. 20, no. 26, B244–B249, 2012. DOI: 10.1364/OE.20.00B244.

[11] T. Pfau, "Carrier recovery algorithms and real-time DSP implementation for coherent receivers", in *Optical Fiber Communications Conference and Exhibition (OFC)*, San Francisco, CA, USA, 2014, pp. 1–17. DOI: 10.1364/OFC.2014.W4K.1.

[12] P. Sadeghi, R. A. Kennedy, P. B. Rapajic, and R. Shams, "Finite-state Markov modeling of fading channels-a survey of principles and applications", *IEEE Signal Processing Magazine*, vol. 25, no. 5, pp. 57–80, 2008. DOI: 10.1109/MSP.2008.926683.

[13] E. O. Elliott, "Estimates of error rates for codes on burst-noise channels", *The Bell System Technical Journal*, vol. 42, no. 5, pp. 1977–1997, 1963. DOI: 10.1002/j.1538-7305.1963.tb00955.x.

[14] T. Koike-Akino, D. S. Millar, K. Kojima, and K. Parsons, "Phase noise-robust LLR calculation with linear/bilinear transform for LDPC-coded coherent communications", in *CLEO: Science and Innovations*, San Jose, California United States, 2015, SW1M–3. DOI: 10.1364/CLEO_SI.2015.SW1M.3.

[15] "IEEE Standard for Ethernet Amendment 9: Physical Layer Specifications and Management Parameters for 25 Gb/s and 50 Gb/s Passive Optical Networks, IEEE Std 802.3ca-2020". (2020).

[16] S. Finkler and D. Sidhu, "Performance analysis of IEEE 802.3z Gigabit Ethernet Standard", in *Seamless Interconnection for Universal Services. Global Telecommunications Conference. GLOBECOM'99. (Cat. No.99CH37042)*, Rio de Janeiro, Brazil, 1999, 1302–1306 vol.2. DOI: 10.1109/GLOCOM.1999.829982.